

Computational quantum field theory for fermion pair creation in 2-dimensional curved spacetimes

Mohammed Alkhateeb,^{1,2} James P. Edwards,² and Yves Caudano¹

¹*Research Unit Lasers and Spectroscopies (UR-LLS), naXys & NISM,
University of Namur, Rue de Bruxelles 61, B-5000 Namur, Belgium.*

²*Mathematical Sciences Department, University of Plymouth, Plymouth, PL4 8AA, UK*

Similarly to the well-known phenomenon of particle / anti-particle pair production in strong electromagnetic fields (the Schwinger effect), the naïve matter field vacuum state can be excited by time-dependent, curved spacetime geometries. This gravitational pair creation corresponds to tunnelling out of a false vacuum. In this work, we study this non-perturbative process using a spacetime resolved numerical approach in the interaction picture. To achieve this, we extend the framework of Computational Quantum Field Theory (CQFT), which allows for efficient numerical time evolution of quantum fields, to spin-1/2 fermions in curved spacetime.

Using this extended framework, we investigate vacuum excitation of a Dirac field induced by a spacetime-curvature quench. In particular, we evolve the fermionic Minkowski vacuum in a 1+1-dimensional idealized curved spacetime characterized by a localized “curvature bump” generated by a smooth, localized Gaussian deformation of flat spacetime. Vacuum excitation is quantified by computing the fermion–antifermion pair numbers defined with respect to the basis corresponding to flat-spacetime (Minkowski) which is the asymptotic metric corresponding to an observer at infinity.

We analyze how the excitation depends on the strength and spatial extent of the curvature deformation and discuss the numerical implementation of CQFT in curved backgrounds. While the post-quench geometry considered here is static and no electromagnetic field is included, the present work establishes a foundation for future investigations of particle creation in genuinely time-dependent curved spacetimes and in the presence of electromagnetic backgrounds.

I. INTRODUCTION

The creation of particle-antiparticle pairs from the vacuum under strong electromagnetic fields was studied from a field theory perspective by Schwinger [1], who used the quantum electrodynamics of fermions with an electric field background. Schwinger’s work builds upon earlier work of Sauter, who solved the Dirac equation in a classical electric field background [2], alluding to the possibility of particle–antiparticle pair creation. In particular, Sauter identified transitions between positive- and negative-energy states induced by potential ramps of the order of the rest energy over distances comparable to the Compton wavelength. An elegant route to determining the pair creation rate, via the optical theorem, was provided by the calculation of the imaginary part of the effective action of by Euler and Heisenberg (spinor QED) [3] and Weisskopf (scalar QED) [4]. The Schwinger effect can be understood as a tunneling process out of a false vacuum, and so is exponentially suppressed below a “critical” electric field strength, $1.3 \times 10^{18} \text{ V/m}$. Such field strengths still cannot be reached in earth-based experiments such as at high-intensity laser facilities (in the lab frame), although the field strengths experienced in the rest frame of a highly Lorentz-boosted electron incident on current and next-generation lasers can in fact surpass this critical field [5–8].

A similar effect was later predicted by Hawking [9, 10], where strong gravitational fields near the event horizon of black holes lead to the creation of particle-antiparticle pairs. In this case, the curved spacetime background plays a role analogous to the electric field

in the Schwinger effect, giving rise to what is known as Hawking radiation. Another famous example, the Unruh effect, can similarly be associated with the appearance of a horizon in the spacetime of a uniformly accelerated observer [11–13]. The success of quantum field theory in curved spacetimes in predicting Hawking radiation has inspired further studies in the emerging field of gravity analogs, including optical [14, 15] and acoustic [16, 17] analogs of black holes, as well as black hole analogs in condensed matter systems [18, 19].

In the context of studying pair production in strong electromagnetic fields in flat spacetimes, computational quantum field theory (CQFT) has proven successful in studying the creation of electron-positron pairs resulting from colliding laser pulses where the calculation of electron and positron densities is performed by evolving the fermionic vacuum state in the presence of a time-dependent background field [20–23]. CQFT has also been successful in understanding the dynamics of Klein tunneling [24–26] and has provided insights into the tunneling time problem [27, 28]. The extension of the framework of CQFT to curved spacetime seems natural given this success, and is the subject of this work. Indeed, doing so would align the CQFT framework with recent studies of pair creation in combined electromagnetic and gravitational fields [29–33].

The mechanism of particle creation by time-dependent and spatially varying gravitational backgrounds has been extensively studied within the framework of quantum field theory in curved spacetime [34, 35]. Well-known examples include cosmological particle production during inflation [36, 37] and Hawking radiation from black

holes [9, 38]. In these settings, standard analytic techniques employed include Bogoliubov transformations relating asymptotic in- and out-mode [9, 34–37, 39, 40], as well as adiabatic renormalization schemes [41]. Alternatives, based on saddle points [42–44] in the worldline formalism of quantum field theory [45, 46] and the double copy [47–50] have also been applied. These semiclassical approaches provide deep conceptual insight but rely on adiabaticity or the existence of well-defined asymptotic regions, making them less suitable to account for the dynamics in the regions of localized curvature structures, or during the rapid changes of geometries, or in the situations lacking global Killing vectors.

On the numerical side, several methods have been developed to solve the Dirac equation in curved or effectively curved geometries. In the context of Dirac materials, quasiconformal coordinate transformations have been used to simulate electron dynamics on strained graphene surfaces, where strain induces an effective curved metric [51]. In addition, pseudospectral and operator-splitting techniques have been introduced to treat Dirac Hamiltonians with spatially varying coefficients with high accuracy [52]. These approaches focus on the single-particle Dirac equation, whereas the present work extends this line of research to the second-quantized Dirac field and investigates the nonperturbative vacuum excitation and pair creation induced directly by space-time curvature within the CQFT framework.

The present work contributes to this landscape by extending the computational quantum field theory (CQFT) approach [20, 21, 23] to curved spacetimes. CQFT evolves the fermionic field state in real time by recasting this evolution as generated by the first quantized Dirac Hamiltonian. This is simulated on a discretized space-time lattice by constructing the time evolution using the split-operator approach to avoid the doubling problem corresponding to spurious fermion modes caused by lattice discretization [53]. Unlike the Bogoliubov transformations between in and out states that yield expectation values of observables in the asymptotic regime, the CQFT framework employed here enables the direct evaluation of time-dependent and spatially resolved observables at finite times throughout the evolution.

One challenge in CQFT is the well-known ambiguity of particle number at transient times (see, for example [54]). The expectation value of the particle number (or density) operator, or the contribution to this expectation value from states with given momentum and spin labels, is in general dependent on the basis of one-particle states used to define these (second quantized) operators. This reflects the inequivalence of the asymptotic vacua (and indeed that of the instantaneous Hamiltonian) which lead to different mode decompositions of the field – which also shows pair creation to be down to vacuum decay. For example, when particle numbers are computed using a mode expansion in terms of adiabatic eigenstates of the Dirac equation built from the vacuum state in the asymptotic future, the resulting particle numbers

at a given time correspond to those that would be observed asymptotically if the external background were removed instantaneously [54]; these numbers can vary across a range orders of magnitude larger than the physical, asymptotic number of created pairs. To mitigate this ambiguity, calculations are typically performed in field configurations that vanish asymptotically in space or time, where an unambiguous particle interpretation in terms of free asymptotic states is available far from the interaction region [26–28]. Similarly, in the present work, the extended CQFT framework for curved spacetimes is applied to backgrounds that are asymptotically flat. Importantly, however, a central advantage of CQFT is its ability to evaluate real-time, spatially or momentum resolved observables, such as charge densities and currents, at finite times and in arbitrary background fields, independently of a specific particle interpretation.

The approach introduced in this work provides the possibility of real-time, operator-level simulation of fermionic vacuum excitation in a genuinely curved spacetime background using a numerically tractable split-operator method. The approach therefore opens a complementary pathway for investigating nonperturbative quantum field-theoretical phenomena in curved spacetimes, with a level of dynamical and operator-level control that is difficult to obtain in existing numerical frameworks. In particular, we implement the quantum field theory of the Dirac field in a genuinely curved 1+1-dimensional spacetime and demonstrate that spacetime curvature alone—without electromagnetic fields—can induce quench-driven vacuum excitation and fermion-antifermion pair production with respect to a chosen mode decomposition, visible in the real-time evolution of the vacuum.

Our formalism integrates the covariant Dirac equation, the spin connection, and curvature-dependent Hamiltonian into a numerically stable operator-splitting scheme. This places our approach at the intersection of semiclassical QFT in curved backgrounds, strong-field QED numerics, and analogue-gravity simulations. The resulting framework provides a complementary, nonperturbative tool to investigate particle creation in arbitrary time-dependent geometries, accounting for the dynamics inside the regions of localized curvature profiles. In order to investigate quantum effects in curved spacetimes with considerably lower computational cost, it is common to reduce the dimensionality of the problem as we do here, although the method proposed is not restricted to lower space-time dimension.

Dilaton gravity [55–59] provides a string-inspired framework [55] in which such a dimensional reduction can be carried out while retaining essential gravitational features. In the present work, the spacetime metric is not assumed to be a solution of a specific dilaton gravity model; rather, it is inspired by dilaton-type geometries, and is chosen to provide a smooth and nonsingular curved background suitable for studying vacuum excitation and particle creation within the CQFT framework.

The paper is organized as follows. Section II reviews the CQFT formalism in flat spacetime and the split-operator implementation used throughout. In Sec. III we extend this framework to a 1+1-dimensional curved background described by a smooth, localized Gaussian deformation of flat spacetime, and derive a Hermitian Hamiltonian together with a unitary time-evolution operator. Section IV presents numerical results for the real-time evolution of the fermionic vacuum in this deformed spacetime and the associated pair-production observables. Finally, Sec. V discusses the physical interpretation and limitations of the particle-number definition used here and outlines extensions of the approach to more realistic measurement scenarios and additional external fields.

II. FORMALISM OF COMPUTATIONAL QUANTUM FIELD THEORY

We begin with a brief review of the CQFT approach for electromagnetic interactions on a flat spacetime before then adapting this formalism to a curved manifold. As such we will present the Dirac equation in the context of both relativistic quantum mechanics and quantum field theory before outlining the connection between the two.

A. First-quantized Dirac theory

In flat spacetime, the Dirac equation for a relativistic particle in the presence of an external electromagnetic four-potential $A_\mu(x)$ reads

$$(i\gamma^\mu D_\mu(x) - m)\psi(x) = 0, \quad (1)$$

$$D_\mu = \partial_\mu - iA_\mu \quad (2)$$

where natural units $\hbar = c = e = 1$ are used throughout this work. Here $x^\mu = (t, \mathbf{x})$ denotes the spacetime coordinates with $\mu = 0, 1, 2, 3$ and $A_\mu(x)$ represents a prescribed (fixed and classical) external electromagnetic background. In a chosen inertial frame, this equation can be rewritten in Schrödinger form as

$$i\partial_t\psi(t, \mathbf{x}) = (\hat{H}_{fr} + \hat{H}_{em})\psi(t, \mathbf{x}), \quad (3)$$

$$\hat{H}_{em} = \gamma^0\gamma^\mu A_\mu \quad (4)$$

where \hat{H}_{fr} is the free Dirac Hamiltonian and \hat{H}_{em} represents the electromagnetic interaction with the field.

We now specialize to fermionic field theory in $1 + 1$ spacetime dimensions. In this case one may choose the following representation of the Clifford algebra,

$$\gamma^0 = \sigma_3, \quad \gamma^1 = i\sigma_2,$$

which leads to the free Hamiltonian

$$\hat{H}_{fr} = \hat{p}\sigma_1 + m\sigma_3. \quad (5)$$

In the following, we take x to denote the spatial coordinate and t the temporal coordinate in the laboratory

frame. The first quantized version of this theory – or the one-particle theory – has, of course, various well-known issues. However, we presented it here because the Hamiltonian in equation (3) will reappear when we reformulate the second quantized theory below.

In the single particle theory, the Dirac equation is considered as applying to the wavefunction, $\psi(x)$. The Hilbert space is spanned by eigenstates of \hat{H}_{fr} , which are easily expressed in position space in terms of the familiar (2D) Dirac spinors:

$$\nu_p(x) = N(p) \begin{pmatrix} \frac{1}{p} \\ \frac{m + E_p}{m + E_p} \end{pmatrix} e^{-ipx},$$

$$\omega_p(x) = N(p) \begin{pmatrix} -\frac{p}{m + E_p} \\ 1 \end{pmatrix} e^{ipx}.$$

In the above, x is the spatial coordinate, and $\nu_p(x)$ and $\omega_p(x)$ are the positive and negative frequency wavefunctions of the one-particle Hamiltonian.

B. Second quantization and QFT observables

In the second-quantized theory, the fermionic field is promoted to an operator, expanded as as

$$\hat{\psi}(t, x) = \int dp \left(\hat{b}_p(t) v_p(x) + \hat{d}_p^\dagger(t) w_p(x) \right), \quad (6)$$

where $v_p(x)$ and $w_p(x)$ are the positive- and negative-energy solutions of the free Dirac equation, and $\hat{b}_p(t)$ and $\hat{d}_p^\dagger(t)$ are the fermionic annihilation operators for particles and antiparticles, respectively – these obey the standard anti-commutation relations for creation and annihilation operators and are used to build the Fock space of multi-particle states of the field.

The quantum-field-theoretical Hamiltonian is

$$\hat{\mathcal{H}} = \hat{\psi}^\dagger(t, x) \hat{H} \hat{\psi}(t, x), \quad (7)$$

where \hat{H} is the corresponding first-quantized Hamiltonian in (3). The connection between the second quantised approach and the first quantised Schrödinger form presented above is that it has been shown [21] that the Heisenberg equation of motion for the field operator,

$$i\partial_t\hat{\psi}(t, x) = [\hat{\psi}(t, x), \hat{\mathcal{H}}], \quad (8)$$

can be written (*exactly*) similarly to the single-particle evolution equation

$$i\partial_t\hat{\psi}(t, x) = \hat{H} \hat{\psi}(t, x). \quad (9)$$

Here, the Hamiltonian \hat{H} acts on the spinor-valued mode functions appearing in the expansion of the field operator. Consequently, the time evolution of the field operator can

be generated by an operator, $\hat{U}(t)$, interpreted in the first quantized setting,

$$\hat{\psi}(t, x) = \hat{U}(t) \hat{\psi}(0, x) = e^{-i\hat{H}t} \hat{\psi}(0, x), \quad (10)$$

where the final equality holds for stationary one-particle Hamiltonians.

The time dependence of the creation and annihilation operators is obtained by re-expanding the evolved field operator in a fixed reference basis, chosen according to the physical context of the measurement. In the presence of external electromagnetic fields that vanish asymptotically in space or in time¹, a natural choice for this basis is the set of free Dirac eigenstates. Hence we can write

$$\begin{aligned} \hat{b}_p(t) &= \int dp' \left(U_{v_p v_{p'}}(t) \hat{b}_{p'} + U_{v_p w_{p'}}(t) \hat{d}_{p'}^\dagger \right), \\ \hat{d}_p^\dagger(t) &= \int dp' \left(U_{w_p v_{p'}}(t) \hat{b}_{p'} + U_{w_p w_{p'}}(t) \hat{d}_{p'}^\dagger \right), \end{aligned} \quad (11)$$

where, for example, our matrix notation means

$$U_{w_p v_{p'}}(t) = \int dx v_p^\dagger(x) \hat{U}(t) w_{p'}(x),$$

and \hat{b}_p , \hat{d}_p are the annihilation operators in the asymptotic past (in our scenario of a curvature quench this is equivalent to taking the operators at $t = 0$), and similarly for creation operators. So the time-evolved operators define a Fock space in terms of the creation and annihilation operators in the asymptotic past.

With these identifications, the number-density operators associated with positive- and negative-energy states are defined as

$$\begin{aligned} \hat{\rho}_+(t, x) &= \iint dp dp' \hat{b}_p^\dagger(t) \hat{b}_{p'}(t) v_p^\dagger(x) v_{p'}(x), \\ \hat{\rho}_-(t, x) &= \iint dp dp' \hat{d}_p^\dagger(t) \hat{d}_{p'}(t) w_{p'}^\dagger(x) w_p(x). \end{aligned} \quad (12)$$

Note that this definition implicitly contains the identification of particle states according to the time-evolved operators. The momentum spectrum of the created fermions (respectively anti-fermions) is determined by the number operators corresponding to each particle momentum,

$$\begin{aligned} \hat{\rho}_{p+}(t, p) &= \hat{b}_p^\dagger(t) \hat{b}_p(t) \\ \hat{\rho}_{p-}(t, p) &= \hat{d}_p^\dagger(t) \hat{d}_p(t). \end{aligned} \quad (13)$$

Similarly, the charge-density operator is given by

$$\hat{\rho}(t, x) = \hat{\psi}^\dagger(t, x) \hat{\psi}(t, x). \quad (14)$$

Inserting the mode expansion only the particle and antiparticle (“diagonal”) terms will survive once we take vacuum expectation values below. Using the fermionic anti-commutation relations, one finds

$$\begin{aligned} \hat{\rho}(t, x) &= \iint dp dp' \hat{b}_p^\dagger(t) \hat{b}_{p'}(t) v_p^\dagger(x) v_{p'}(x) \\ &\quad - \iint dp dp' \hat{d}_p^\dagger(t) \hat{d}_{p'}(t) w_p^\dagger(x) w_{p'}(x) + \dots \\ &= \hat{\rho}_+(t, x) - \hat{\rho}_-(t, x) + \dots \end{aligned} \quad (15)$$

where the omitted terms will drop out below.

To determine a number or charge density of created pairs in the Heisenberg picture, we determine the vacuum expectation values of $\hat{\rho}_+$, $\hat{\rho}_-$, and $\hat{\rho}_p$, obtaining, respectively:

$$\begin{aligned} \rho_+(t, x) &= \int dp \left| \int dp' U_{v_p w_{p'}}(t) v_p(x) \right|^2 \\ \rho_-(t, x) &= \int dp \left| \int dp' U_{w_p v_{p'}}(t) w_p(x) \right|^2 \\ \rho_{p+}(t, p) &= \int dp' \left| U_{w_p v_{p'}}(t) \right|^2 \\ \rho_{p-}(t, p) &= \int dp' \left| U_{v_p w_{p'}}(t) \right|^2. \end{aligned} \quad (16)$$

However, ρ_\pm can only be interpreted unambiguously as corresponding to the *physical* density of pairs created in the asymptotic limit $t \rightarrow \infty$, or at large spatial distances from variation in the electromagnetic field profile. This is because these expectation values depend explicitly on the choice of basis (through $v_p(x)$ and $w_p(x)$), or, physically, the choice of states that fill out the Fock space and define the multi-particle states.

C. Split-operator approach to Computational Quantum Field Theory Evolution

The CQFT approach aims to evaluate observables at successive times during the real-time evolution of the Dirac field operator generated by the first quantized Hamiltonian with a finite spatial resolution. In order to do so, we discretize space to a one-dimensional lattice of width Λ ,

$$X = \left\{ -\frac{N}{2} \delta x, \left(-\frac{N}{2} + 1 \right) \delta x, \dots, \frac{N}{2} \delta x \right\},$$

with lattice spacing $\delta x = \Lambda/(N+1)$. The corresponding reciprocal-space lattice is

$$P = \left\{ -\frac{N}{2} \delta p, \left(-\frac{N}{2} + 1 \right) \delta p, \dots, \frac{N}{2} \delta p \right\},$$

where $\delta p = 2\pi/\Lambda$.

¹ The extension to gauge potentials that are asymptotically constant is straightforward

The background scalar potential $V(x)$ and vector potential $A(x)$ are evaluated on the position-space lattice, while the free Hamiltonian \hat{H}_{fr} is most conveniently evaluated in momentum space. For each momentum $p = n\delta p$, with $n \in \{-\frac{N}{2}, -\frac{N}{2} + 1, \dots, \frac{N}{2}\}$, the (first quantised) positive- and negative-energy basis spinors are the momentum space eigenstates of H_{fr} :

$$\langle p|v_p\rangle = N(p) \begin{pmatrix} 1 \\ \frac{p}{m+E_p} \end{pmatrix},$$

$$\langle p|w_p\rangle = N(p) \begin{pmatrix} \frac{p}{m+E_p} \\ 1 \end{pmatrix},$$

where $E_p = \sqrt{p^2 + m^2}$ and $N(p)$ is a normalization factor.

The time-evolution operator over a short time step δt is written in symmetrized (second-order) split-operator form as

$$\hat{U}(\delta t) = \hat{U}_{em} \left(\frac{\delta t}{2} \right) \hat{U}_{fr}(\delta t) \hat{U}_{em} \left(\frac{\delta t}{2} \right), \quad (17)$$

where U_{fr} and U_{em} denote the evolution operators associated with the free Hamiltonian and the electromagnetic interaction, respectively. The matrix element of the free evolution operator is given explicitly by

$$\langle p'|\hat{U}_{fr}(\delta t)|p\rangle = \langle p'|e^{-i\hat{H}_{fr}\delta t}|p\rangle = \begin{pmatrix} U_{11} & U_{12} \\ U_{21} & U_{22} \end{pmatrix} \delta(p - p'), \quad (18)$$

with matrix elements

$$U_{11} = \cos(E_p\delta t) - i\frac{m}{E_p} \sin(E_p\delta t),$$

$$U_{12} = -i\frac{p}{E_p} \sin(E_p\delta t), \quad (19)$$

$$U_{21} = U_{12},$$

$$U_{22} = \cos(E_p\delta t) + i\frac{m}{E_p} \sin(E_p\delta t).$$

The interaction step is applied in position space and reads

$$\langle x'|\hat{U}_{em}(\tau)|x\rangle = \exp[-i(V(x) + \sigma_1 A(x))\tau] \delta(x - x'). \quad (20)$$

Transition amplitudes such as $U_{w_p v_p} \equiv \langle w_p|\hat{U}|v_p\rangle$, $U_{w_p w'_p} \equiv \langle w_p|\hat{U}|w'_p\rangle$ and so on, are evaluated numerically. With these in hand, we can then evaluate the created pair number and / or charge densities by evaluating (16) on the discretised momentum space lattice.

The same CQFT approach presented in this section can be used to calculate the numbers and number densities of created boson-antiboson pairs and to study the propagation of bosonic wave packets in strong electromagnetic fields that are supercritical with respect to the bosonic mass [60, 61].

This approach has been used to study the dynamics of Klein tunneling [26] and regular tunneling of both

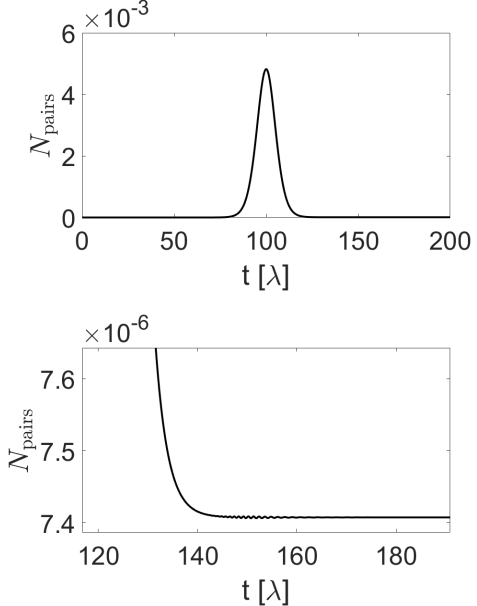


FIG. 1. Number of created fermion-antifermion pairs for a Sauter step given by Eq. (21), with $E_0 = 1/4$, and $\omega = 0.1$. The upper panel shows the time evolution over a duration of 200λ , while the lower panel is a zoom of the late-time region. The obtained asymptotic number is $N \simeq 7.4 \times 10^{-6}$. The calculation is performed using CQFT on a lattice of width 100λ with 2^{11} sites and time step $\delta t = 0.001\lambda$ increasing the number of lattice sites or reducing the time step does not change the curves at the resolution shown. The asymptotic number of created pairs agrees with the asymptotic adiabatic particle number [54].

fermionic and bosonic fields [62], where the background field vanishes asymptotically and inside the potential barrier through which the propagation of the tunneled wave packet takes place. For this reason, the same re-expansion as in Eq. (11) was used in those works. However, in other contexts where the background field is time dependent, different re-expansions can be employed. For example, one may use a basis that diagonalizes the Hamiltonian instantaneously. This yields the same particle numbers as those obtained from the adiabatic particle number at late times.

As an illustration, for a Sauter time-dependent field,

$$a(t) = \frac{E_0}{\omega} (1 + \tanh(\omega t)), \quad (21)$$

one can use the basis that diagonalizes the Hamiltonian given in Eq. (3) either instantaneously or at late times and recover the same particle number as obtained using the adiabatic particle number [54], as shown in Fig. 1.

III. COMPUTATIONAL QUANTUM FIELD THEORY IN CURVED SPACETIMES

To adapt CQFT to curved spacetime we will start with the Dirac equation and show that (at least in (1+1)-dimensional spacetime) it can be recast into Schrödinger form. We will then show that the first-quantized quantum theory can be used to generate time evolution for the second quantized theory as for electromagnetic interactions – although achieving this will require a field definition. For details on our curved space conventions see Appendix A.

In curved spacetime, the free massive Dirac equation takes the covariant form (see (A 6))

$$i\gamma^\nu(x)\nabla_\nu\psi(x) - m\psi(x) = 0, \quad (22)$$

where ∇_ν denotes the spinor covariant derivative. Using the vielbein formalism, whereby we set $g_{\mu\nu}(x) = e_\mu^a(x)e_\nu^b(x)\eta_{ab}$ and $\gamma^\mu = e^\mu_a\gamma^a$, this equation can be written explicitly as

$$ie^\nu_a(x)\gamma^a(\partial_\nu + \Omega_\nu(x))\psi(x) - m\psi(x) = 0, \quad (23)$$

where e^ν_a are the vielbeins and Ω_ν is the spinor connection (Fock–Ivanenko coefficient) detailed further below.

Throughout this section, we distinguish between curved spacetime coordinates (τ, ξ) and local Lorentz (tangent-space) coordinates (t, x) , and we will use the Greek letters corresponding to the curved coordinates instead of their respective numerical indices when citing the connections and tetrads. For example, we will use $\Gamma_{\tau\xi}^\xi$ and $e^\tau{}_0$ rather than Γ_{01}^1 and $e^0{}_0$ so that the curved coordinate variable is indicated explicitly.

Background geometry

We consider a static 1+1-dimensional spacetime that is flat Minkowski space for $\tau < 0$. We introduce a deformation for $\tau \geq 0$, whereby the manifold becomes curved, with line element

$$ds^2 = \alpha(\xi)d\tau^2 - \frac{d\xi^2}{\alpha(\xi)}, \quad (24)$$

where

$$\alpha(\xi) = 1 - \beta e^{-\xi^2/r_0^2}. \quad (25)$$

Here, then, r_0 controls the width of the Gaussian deformation of flat spacetime and β control its strength. In order to avoid coordinate singularities and keep the metric signature fixed, we choose to take β to be smaller than unity.

The metric (24) is chosen as a smooth, asymptotically flat deformation of flat spacetime that is free of curvature singularities. Such regular background geometries are particularly well suited for numerical investigations of

quantum field dynamics in curved spacetime. Although no assumption is made regarding the microscopic gravitational origin of this geometry, the metric Eq. (24) is inspired by a classical solution of a 2-dimensional string theory [55, 58] where the metric takes the same form as in Eq. (24) with $\alpha(\xi) = 1 - \beta e^{-Q\xi}$.

This restriction to smooth spacetimes is motivated by fundamental considerations in quantum field theory on curved backgrounds. In spacetimes containing curvature singularities or lacking global hyperbolicity, the quantum Hamiltonian governing field evolution generally fails to be essentially self-adjoint. As a consequence, quantum time evolution is not uniquely defined unless additional boundary conditions are specified at the singularity, leading to ambiguities in the dynamics [63]. By working with a regular background geometry that is asymptotically flat, these issues are avoided and a well-defined, unitary time evolution will ensue (see below).

The non-vanishing Christoffel symbols associated with the metric (24) are (see Appendix A 2)

$$\begin{aligned} \Gamma_{\xi\tau}^\tau &= \Gamma_{\tau\xi}^\tau = \frac{\alpha'(\xi)}{2\alpha(\xi)}, \\ \Gamma_{\tau\tau}^\xi &= \frac{1}{2}\alpha(\xi)\alpha'(\xi), \\ \Gamma_{\xi\xi}^\xi &= -\frac{\alpha'(\xi)}{2\alpha(\xi)}, \end{aligned} \quad (26)$$

where a prime denotes differentiation with respect to ξ . From here one finds a non-zero Riemann curvature tensor characterised by the Ricci scalar,

$$R(\xi) = \alpha''(\xi) = \frac{2\beta}{r_0^4} e^{-\xi^2/r_0^2} (r_0^2 - 2\xi^2), \quad \tau > 0 \quad (27)$$

(with the Kretschmann scalar being the square of this). This confirms that the metric remains flat at asymptotic spatial distance (recall that in (1+1)-dimensional spacetime the Ricci tensor is given by $R_{\mu\nu}(\xi) = \frac{1}{2}R(\xi)g_{\mu\nu}(\xi)$).

Vielbeins and spin connection

We choose the diagonal vielbein (see Appendix A 1)

$$e^\tau{}_0 = \frac{1}{\sqrt{\alpha(\xi)}}, \quad e^\xi{}_1 = \sqrt{\alpha(\xi)}, \quad (28)$$

with all other components vanishing.

The only non-vanishing components of the spin connection are (see Appendix A 3 and A 4)

$$\omega_{1\tau}^0 = \omega_{0\tau}^1 = \frac{\alpha'(\xi)}{2}, \quad (29)$$

while $\omega_{b\xi}^a = 0$. Then the spinor connection for the matter field is given by (see Appendix A 5)

$$\Omega_\nu = -\frac{i}{4}\omega_{ab\nu}\sigma^{ab}, \quad \sigma^{ab} = \frac{i}{2}[\gamma^a, \gamma^b]. \quad (30)$$

Using the 1+1-dimensional representation $\gamma^0 = \sigma_3$ and $\gamma^1 = i\sigma_2$, one finds

$$\Omega_\tau = \frac{\alpha'(\xi)}{4} \sigma_1, \quad \Omega_\xi = 0. \quad (31)$$

Dirac equation and Hamiltonian formulation

Inserting Eqs. (28) and (31) into (23), the Dirac equation in our curved spacetime becomes (for $\tau > 0$)

$$\begin{aligned} & \frac{i}{\sqrt{\alpha(\xi)}} \sigma_3 \left(\partial_\tau + \frac{\alpha'(\xi)}{4} \sigma_1 \right) \psi(\tau, \xi) \\ & - \left(\sqrt{\alpha(\xi)} \sigma_2 \partial_\xi + m \right) \psi(\tau, \xi) = 0. \end{aligned} \quad (32)$$

The covariant Dirac current $j^\mu = \bar{\psi} \gamma^\mu \psi$ satisfies $\nabla_\mu j^\mu = 0$ and defines a conserved inner product on a Cauchy surface of constant τ . Taking the curvature into account, this inner product is defined by

$$(\psi_1, \psi_2) = \int d\xi \frac{1}{\sqrt{\alpha(\xi)}} \psi_1^\dagger \psi_2. \quad (33)$$

Our aim is to rewrite the equation of motion for the field in Schrödinger form so as to develop a first quantised representation of its time evolution. Nevertheless, the Dirac Hamiltonian obtained from Eq. (32) is not manifestly Hermitian with respect to the flat $L^2(d\xi)$ norm due to the ξ -dependence of the vielbeins. We therefore perform the field redefinition

$$\chi(\tau, \xi) = \alpha^{-\frac{1}{4}}(\xi) \psi(\tau, \xi) \quad (34)$$

which yields a Hamiltonian that is Hermitian with respect to the standard flat inner product

$$(\chi_1, \chi_2) = \int d\xi \chi_1^\dagger \chi_2. \quad (35)$$

In the first quantised setting, the Dirac equation, Eq (32), can then be rewritten in the Schrödinger form in terms of the rescaled field,

$$i\partial_\tau \chi(\tau, \xi) = \hat{H} \chi(\tau, \xi), \quad (36)$$

where τ denotes the curved-spacetime time coordinate associated with the background metric (24). The Hamiltonian is (for $\tau > 0$)

$$\hat{H} = \frac{1}{2} \{ \alpha(\xi), \hat{p} \} \sigma_1 + \sqrt{\alpha(\xi)} m \sigma_3. \quad (37)$$

The anticommutator ensures Hermiticity of the Hamiltonian operator.

It is convenient to decompose \hat{H} into the free flat-spacetime Hamiltonian \hat{H}_{fr} and curvature-induced corrections:

$$\hat{H} = \hat{H}_{fr} + \hat{H}_{gr} \quad (38)$$

$$\hat{H}_{gr} = \frac{1}{2} \{ \alpha(\xi) - 1, \hat{p} \} \sigma_1 + (\sqrt{\alpha(\xi)} - 1) m \sigma_3. \quad (39)$$

For the metric (24), this yields

$$\hat{H} = \hat{H}_{fr} - \frac{1}{2} \{ \beta e^{-\xi^2/r_0^2}, \hat{p} \} \sigma_1 + (\sqrt{1 - \beta e^{-\xi^2/r_0^2}} - 1) m \sigma_3. \quad (40)$$

the free part of the Hamiltonian can be used to define the states of the theory corresponding to flat space.

It is important to note, however, that a rescaling analogous to that introduced in Eq. (34) can be carried out in the general 1+1-dimensional case once the spacetime metric is written in conformally flat form. Indeed, every two-dimensional Lorentzian metric is locally conformally flat. Consequently, a metric of the general form

$$ds^2 = \alpha_1(\tau, \xi) d\tau^2 - \alpha_2(\tau, \xi) d\xi^2 \quad (41)$$

can always be brought, by a suitable local coordinate transformation, to the form (See App. B)

$$ds^2 = \alpha(\tau', \xi') (d\tau'^2 - d\xi'^2). \quad (42)$$

In these conformal coordinates, the spin connection components can be computed straightforwardly. In the representation $\gamma^0 = \sigma_3$ and $\gamma^1 = i\sigma_2$, one finds

$$\Omega_{\tau'} = \frac{\partial_{\xi'} \alpha(\tau', \xi')}{4 \alpha(\tau', \xi')} \sigma_1, \quad \Omega_{\xi'} = \frac{\partial_{\tau'} \alpha(\tau', \xi')}{4 \alpha(\tau', \xi')} \sigma_1. \quad (43)$$

Introducing the rescaled spinor field

$$\phi(\tau', \xi') = \alpha^{1/4}(\tau', \xi') \psi(\tau', \xi'), \quad (44)$$

the Dirac equation assumes the Schrödinger-like form

$$i\partial_{\tau'} \phi(\tau', \xi') = -i \sigma_1 \partial_{\xi'} \phi(\tau', \xi') + m \sqrt{\alpha(\tau', \xi')} \sigma_3 \phi(\tau', \xi'). \quad (45)$$

The corresponding Hamiltonian operator is manifestly Hermitian with respect to the flat inner product, and the resulting time evolution is unitary.

A. Field quantisation and split-operator time evolution

Now we quantise the fields, by setting

$$\hat{\chi}(\tau, \xi) = \int dp \left(\hat{b}_p(\tau) v_p(\xi) + \hat{d}_p^\dagger(\tau) w_p(\xi) \right), \quad (46)$$

where $v_p(x)$ and $w_p(x)$ are the solutions of the free Dirac equations in the Malinowski flat spacetime.

As in flat space, the second quantized Hamiltonian density is

$$\hat{\mathcal{H}} = \hat{\chi}^\dagger(\tau, \xi) \hat{H} \hat{\chi}(\tau, \xi), \quad (47)$$

and the Heisenberg equation for the time evolution of the field can, again, be written using the first quantised Hamiltonian as

$$i\partial_\tau \hat{\chi}(\tau, \chi) = \hat{H} \hat{\chi}(\tau, \chi). \quad (48)$$

As such, we may employ the time evolution operator corresponding to the single-particle Hamiltonian.

The free evolution operator for $\hat{\chi}$ is identical to that obtained in the flat-spacetime case discussed in Sec. II, with the Minkowski time coordinate t replaced by the curved-spacetime time coordinate τ :

$$\hat{U}_{fr}(\delta\tau) = e^{-i\hat{H}_{fr}\delta\tau}. \quad (49)$$

Its explicit matrix representation is therefore not repeated here.

Using a symmetric Baker–Campbell–Hausdorff split-operator scheme, the full time-evolution operator is approximated to $\mathcal{O}(\delta\tau^3)$ as

$$\hat{U}(\delta\tau) = \hat{U}_{cur2}\left(\frac{\delta\tau}{2}\right) \hat{U}_{cur1}\left(\frac{\delta\tau}{2}\right) \hat{U}_{fr}(\delta\tau) \hat{U}_{cur1}\left(\frac{\delta\tau}{2}\right) \hat{U}_{cur2}\left(\frac{\delta\tau}{2}\right). \quad (50)$$

Here \hat{U}_{cur1} corresponds to the momentum-dependent curvature term involving $\{e^{-\xi^2/r_0^2}, \hat{p}\}$ and is evaluated most conveniently in momentum space,

$$\hat{U}_{cur1}(\delta\tau) = \exp\left[-\frac{i}{2}\{\hat{f}, \hat{p}\}\sigma_1\delta\tau\right], \quad (51)$$

where $f(\xi) = \beta e^{-\xi^2/r_0^2}$ and the momentum-space matrix elements of \hat{f} are

$$\begin{aligned} \langle p|\hat{f}|p'\rangle &= \int d\xi \langle p|\xi\rangle f(\xi) \langle \xi|p'\rangle \\ &= \frac{1}{2\pi} \int d\xi f(\xi) e^{i(p'-p)\xi}. \end{aligned} \quad (52)$$

On the other hand, \hat{U}_{cur2} is applied in position space,

$$\langle \xi'|\hat{U}_{cur2}(\delta\tau)|\xi\rangle = \exp[-ig(\xi)\delta\tau] \delta(\xi - \xi'), \quad (53)$$

with

$$g(\xi) = (\sqrt{1 - \beta e^{-\xi^2/r_0^2}} - 1)m\sigma_3. \quad (54)$$

The resulting time-evolution operator \hat{U} is used in direct analogy with the flat-spacetime case discussed in Sec. II. In particular, it is applied to evolve the quantized field in time and to compute transition amplitudes between time-evolved single-particle states. These amplitudes are then used to construct the time-dependent creation and annihilation operators and to evaluate expectation values of quantum field observables.

Since the system is initially prepared in the Minkowski vacuum prior to the introduction of the spacetime curvature quench, the initial field operator is the free Dirac field $\hat{\psi}(0, \xi)$ given by Eq. (6) – this provides the boundary condition for $\hat{\chi}(0, \xi)$. The subsequent time evolution can be described equivalently either by the original Dirac equation Eq. (32) or by the rescaled equation Eq. (36). We evolve the latter, because it yields a Hermitian Hamiltonian and unitary time evolution in our first quantised representation.

As in the flat-spacetime formulation, we project the time evolved field onto a reference basis. In the present work, this basis is chosen to be the set of free Dirac eigenstates. This choice is natural for the background geometry considered here, which is asymptotically flat, and allows for a direct interpretation of particles and antiparticles in terms of free asymptotic states.

The **physical** densities are those corresponding to the conserved currents and can be expressed equivalently in terms of the field $\hat{\psi}(t, x)$ or $\hat{\chi}(t, x)$

$$\hat{\rho}_{ch} = \frac{1}{\sqrt{\alpha(\xi)}} \hat{\psi}^\dagger(\tau, \xi) \hat{\psi}(\tau, \xi) = \hat{\chi}^\dagger(\tau, \xi) \hat{\chi}(\tau, \xi) \quad (55)$$

The number density operators for one particle positive energy and negative energy states ρ_+ are respectively:

$$\begin{aligned} \hat{\rho}_+(\tau, \xi) &= \frac{1}{\sqrt{\alpha(\xi)}} \iint dp dp' \hat{b}_p^\dagger(t) \hat{b}_{p'}(t) v_p^\dagger(\xi) v_{p'}(\xi), \\ \hat{\rho}_-(\tau, \xi) &= \frac{1}{\sqrt{\alpha(\xi)}} \iint dp dp' \hat{d}_p^\dagger(t) \hat{d}_{p'}(t) w_p^\dagger(\xi) w_{p'}(\xi), \end{aligned} \quad (56)$$

if these operators are derived from the field decomposition of ψ and

$$\begin{aligned} \hat{\rho}_+(\tau, \xi) &= \iint dp dp' \hat{b}_p^\dagger(\tau) \hat{b}_{p'}(\tau) v_p^\dagger(\xi) v_{p'}(\xi), \\ \hat{\rho}_-(\tau, \xi) &= \iint dp dp' \hat{b}_p^\dagger(\tau) \hat{b}_{p'}(\tau) w_p^\dagger(\xi) w_{p'}(\xi), \end{aligned} \quad (57)$$

if they are derived from the field decomposition of χ . The number density operators in the momentum space are given by

$$\begin{aligned} \hat{\rho}_{p+}(\tau, p) &= \hat{b}_p^\dagger(\tau) \hat{b}_p(\tau) \\ \hat{\rho}_{p-}(\tau, p) &= \hat{d}_p^\dagger(\tau) \hat{d}_p(\tau). \end{aligned} \quad (58)$$

The number density of one-particle states defined with respect to the Minkowski free basis as introduced in Eqs. (56) and (57) are basis dependent and correspond to excitations measured relative to the Minkowski vacuum (this can be shown by calculating the time evolution after turning off the spacetime curvature at any instant such the evolution continues with the free Minkowski space Hamiltonian only whereafter the number density remains constant). In contrast, the charge density operator give by Eq. (55) is a basis-independent observable.

Using the time evolution operator Eq. (50), one can compute the amplitudes $U_{w_p v_p}$, $U_{v_p v'_p}$ and so on. The number density of the created fermion–anti-fermion pairs ρ_{pairs} and their spectrum $\rho_p(p)$, all calculated with respect to the flat spacetime vacuum, are then obtained by computing the vacuum expectation value of $\hat{\rho}_+(\tau, \xi)$ or $\hat{\rho}_-(\tau, \xi)$ given by Eqs. (56). The vacuum expectation values are given by

$$\begin{aligned}
\rho_+(\tau, \xi) &= \int dp \left| \int dp' U_{v_p w_{p'}}(\tau) v_p(\xi) \right|^2 \\
\rho_-(\tau, \xi) &= \int dp \left| \int dp' U_{w_p v_{p'}}(\tau) w_p(\xi) \right|^2 \\
\rho_{p+}(\tau, p) &= \rho_{p-}(\tau, p) = \int dp' \left| U_{w_p v_{p'}}(\tau) \right|^2 \\
&= \int dp' \left| U_{v_p w_{p'}}(\tau) \right|^2.
\end{aligned} \tag{59}$$

while the expectation value of the charge density is vanishing everywhere, as no charge separation is taking place since the spacetime curvature does not couple to charge, and no electromagnetic field is included in the scenarios discussed in this work. The number of pairs N_{pairs} is then obtained by integrating ρ_{pairs} over ξ or by integrating $\rho_p(p)$ over p so that one obtains:

$$N_{\text{pairs}} = \int dp \int dp' \left| U_{v_p w_{p'}}(\tau) \right|^2 \tag{60}$$

It is important to note that in the framework of the CQFT presented in this work the background geometry can be time-dependent as one can introduce space- and time-dependent perturbations to the flat Minkowski vacuum. However, neither the backreaction nor the self-interaction of the matter field is accounted for. The fermionic field is therefore evolved on the background geometry without accounting for gravitational backreaction or fermion self-interactions. The present formulation thus corresponds to quantum field theory on a prescribed classical spacetime. Extensions of the method that incorporate backreaction and self-reaction effects and loop corrections will be considered in future work.

IV. RESULTS AND ILLUSTRATIONS

Starting from the field characterizing the fermionic vacuum, we evolve it using the time evolution operator calculated in the curved spacetime characterized by the Gaussian deformation of the flat spacetime, Eq (24). We calculate the number densities and the spectrum of the created fermions in position space.

In Fig. 2 we show the time evolution of the number density as a function of spatial position, by plotting this density for three illustrative times.

The results show that pair creation is initially supported close to the central, positive peak in the Ricci curvature. Pairs later start to form in regions of negative curvature and propagate outwards. Before saturation, the total number of pairs is monotonically increasing (see also Fig. 3). The part of the density created in the regions of negative curvature gradually propagate far from the center of the curvature bump while the part created in the positive region is confined inside the curvature region, blocking more creation at later times (the

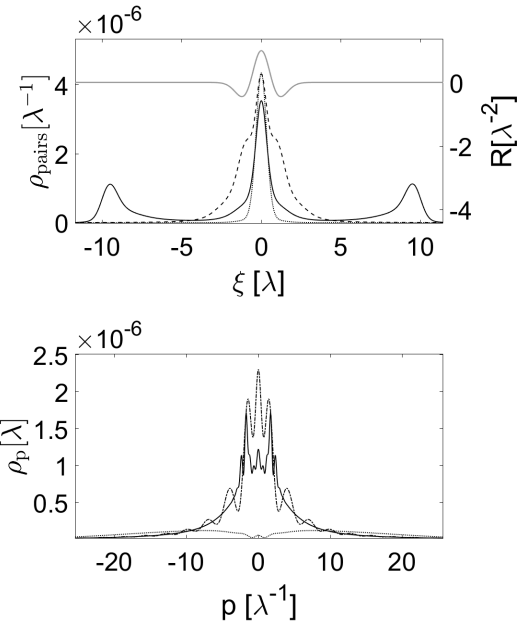


FIG. 2. Number density of created fermion-antifermion pairs (upper panel) and their momentum spectrum (lower panel) at three times: $\tau = 0.1\lambda$ (dotted line), $\tau = 1.3\lambda$ (dashed line), and $\tau = 10\lambda$ (solid black line), where λ is the electron Compton wavelength. The Ricci scalar $R(\xi)$, Eq. (27) corresponding to the spacetime curvature given by Eqs. (24) and (25) with $\beta = \frac{1}{2}$ is shown in the upper panel by the solid gray line. Calculations use $N = 2^{11}$ lattice sites and a time step $\delta\tau = 0.01\lambda$.

Pauli blockade). The momentum spectrum shows little temporal variation of the range of momenta of created pairs, but they become more concentrated about the turning points of the scalar curvature momentum as time increases, which tends to reduce the range of momenta carried by the pairs produced at later times.

In Fig. 3 we plot the total number of created fermion-antifermion pairs as a function of time. After an ini-

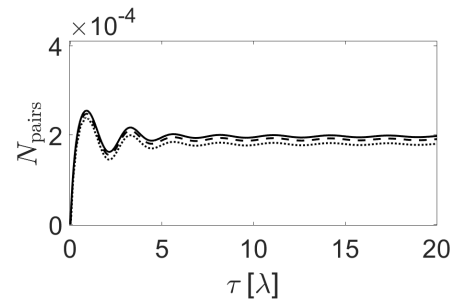


FIG. 3. Number of created pairs in the case of a Gaussian deformation of width $r = 1\lambda$ and lattice width $\Lambda = 100\lambda$ for different lattice spacings corresponding to $N = 2^9$ sites (dotted line), $N = 2^{10}$ (dashed line), $N = 2^{11}$ (solid line). For greater values of N , the curves become indistinguishable in the plotting resolution.

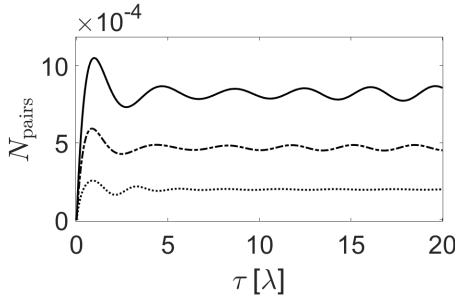


FIG. 4. Number growth of created fermion-antifermion pairs for different widths of the Gaussian curvature Eq. (25). For wider curvatures, the production reaches saturation at later times and for greater numbers of created pairs. The dotted line corresponds to $r_0 = 1\lambda$, the dash-dotted line corresponds to $r_0 = \sqrt{2}\lambda$ and the solid line corresponds to $r_0 = \sqrt{3}\lambda$. The numbers are calculated on a lattice of width 100λ and of $N = 2^{11}$ sites.

tial growth, the production reaches saturation due to the Pauli blocking discussed above. The number of pairs created at which saturation sets in depends on the spatial width of the curvature deformation; wider curvature profiles lead to greater asymptotic pair numbers, as shown in Fig. 4, as the pairs can be excited over a larger spatial volume. Similarly, stronger curvature deformations correspond to larger values of the parameter β in Eq. (25) as it increases the value of the Ricci scalar Eq. (27). As can be seen in Figs. 5 and 6, increasing β results in a faster growth of the particle number and a higher saturation value. Physically, stronger curvature deformations couple to a larger number of fermionic modes, enabling pair production channels that are not accessible for smaller β – note, however, that this does not delay the onset of Pauli blocking.

To assess numerical stability, we performed convergence tests with respect to both the spatial lattice spacing

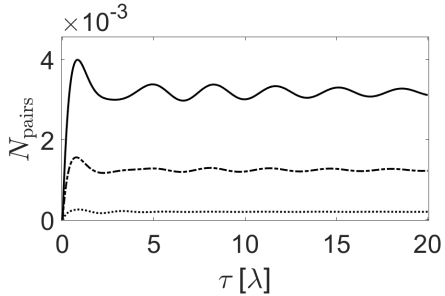


FIG. 5. Number growth of created fermion-antifermion pairs for different strengths of the Gaussian curvature with $r_0 = 1\lambda$. For stronger curvatures, more pairs are created and saturation is reached for greater numbers. The dotted line corresponds to $\beta = 0.5$, the dash-dotted line corresponds to $\beta = 0.7$, the solid line corresponds to $\beta = 0.8$ and the dotted line corresponds to $\beta = 0.9$.

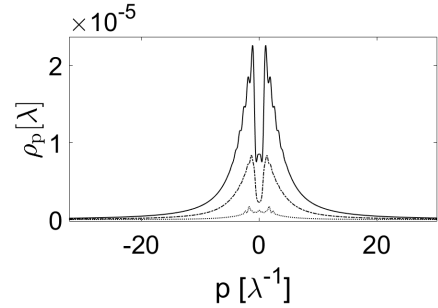


FIG. 6. spectrum of created fermion-antifermion pairs for different strengths of the Gaussian curvature with $r_0 = 1\lambda$. For stronger curvatures, more modes are created and saturation is reached for greater numbers. The solid line corresponds to $\beta = 0.8$ and the dotted line corresponds to $\beta = 0.5$.

$\Delta\xi$ and the time step $\Delta\tau$. For sufficiently small $\Delta\xi$ and $\Delta\tau$ the results for the particle number and spatial number density become indistinguishable within the plotting resolution, indicating that the calculation is in the converged regime. Fig. 3 shows the total number of fermion-antifermion pairs created for several lattice resolutions; convergence is reached for $\Delta\xi \leq 0.097\lambda$ and $\Delta\tau \leq 0.01\lambda$.

As a complementary diagnostic we also monitored the norm of a Gaussian wave packet to test the unitarity of the evolution. Using the time evolution operator, Eq. (50), we evolved a one-particle wave packet propagating through the curved spacetime. The initial wave packet was chosen to be

$$\chi(0, x) = \left(\frac{1}{2\pi\sigma^2} \right)^{1/4} e^{-\frac{(x-x_0)^2}{4\sigma^2}} e^{-ip_0 x} \begin{pmatrix} 1 \\ 0 \end{pmatrix}, \quad (61)$$

with $x_0 = -10\lambda$, $p_0 = 1000\lambda^{-1}$, and $\sigma = 2\lambda$. We found that the symmetrized operator splitting used in Eq. (50) preserves norm to sufficiently high accuracy; over the full simulation time of 20λ the deviation $\epsilon(\tau) = \|\psi(t)\|^2 - 1$ remains below 3.4×10^{-13} for $\delta\xi = 0.0488\lambda$ and $\delta\tau = 0.01\lambda$ and it becomes smaller for smaller $\delta\xi$ and $\delta\tau$. This is consistent with the expected global error of $\mathcal{O}(\delta\tau^2)$ corresponding to an error of $\mathcal{O}(\delta\tau^3)$ over each time step of the second-order splitting scheme. In fig. 7 we show the propagation of this wave packet through the curved spacetime.

V. DISCUSSION

We have shown that the CQFT formalism can be extended to curved spacetimes and used to investigate vacuum excitation and real-time fermion-antifermion pair creation. The particle numbers reported in this work are defined with respect to the free Dirac basis; they correspond to the excitations that would be observed by a Minkowski observer if the curvature were removed instantaneously. As is well known in quantum field theory

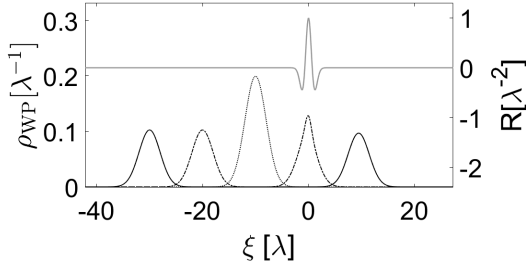


FIG. 7. The probability density of a one-particle fermionic wave packet evolved with the time evolution operator Eq. (50). The initial wave packet is given by Eq. (61) and its corresponding density is shown by the dotted line. The dash-dotted line shows the density corresponding to the evolved wave packet at $t = 10\lambda$, and the solid line shows it at $t = 15\lambda$. The discretization uses a lattice of width 100λ and of 10^{11} sites. The time step is $\delta_t = 0.01\lambda$

in curved spacetime [34, 35], particle number is not an invariant quantity and depends on the particular mode decomposition used to define the vacuum. The goal of the present work is therefore not to provide a physical particle spectrum in a specific observational scenario, but rather to establish the mathematical and numerical framework required for applying CQFT to curved backgrounds and obtain the asymptotic pair creation rate in a given frame.

Another physically meaningful particle definition can be obtained by projecting onto the instantaneous eigenstates of the Hamiltonian or of the charge-density operator; this will be explored in future work. Importantly, while the number densities of separate positive- and negative-energy states depend on the chosen basis, the charge density, which is equal to the difference between them, is basis-independent in the sense that changing the basis corresponds to changing the vacuum with respect to which we calculate the numbers. This becomes especially relevant when spatially dependent electromagnetic fields are included, since they can separate the cre-

ated charges and give rise to basis-independent quantities such as charge densities and currents. The same CQFT approach can be used to investigate the time evolution of scalar fields in curved spacetimes. This will be investigated in future works.

Future extensions of the method will therefore include, in addition to the curved background, spatially varying electromagnetic fields, as well as implementing projection schemes based on instantaneous diagonalization of the Hamiltonian. Additionally, numerical improvements will be implemented to reduce time ordering errors in the time evolution operator beyond the time-step refinement used in the present work [64]. These extensions will enable the study of more realistic physical scenarios in which the notion of particle number becomes unambiguous and directly observable. Moreover, the field selfinteraction can be introduced through effective actions taking into consideration the radiative corrections.

Extending the present CQFT approach to higher spacetime dimensions faces the fact that, in contrast to the two-dimensional case, generic spacetimes are not locally conformally flat. Nevertheless, many physically relevant geometries, including FLRW, de Sitter, and anti-de Sitter spacetimes, are conformally flat. In such cases, rescalings analogous to that introduced in Eq. (34) can be employed to obtain a Hermitian Hamiltonian and a unitary time-evolution operator. By contrast, for spacetimes that are not conformally flat, such as the Schwarzschild geometry, alternative strategies must be adopted, perhaps on a case by case basis, in order to render the Dirac equation in a suitable Schrödinger form so that the first quantised approach can be employed.

ACKNOWLEDGMENTS

M. Alkhateeb acknowledges funding from the European Union's Horizon 2020 research and innovation programme under the Marie Skłodowska-Curie grant agreement No. 101034383. He also thanks the University of Plymouth's hospitality where part of this work was conducted. Y. Caudano is a research associate of the Fund for Scientific Research F.R.S.-FNRS.

[1] J. Schwinger. On gauge invariance and vacuum polarization. *Phys. Rev.*, 82:664–679, Jun 1951.

[2] F. Sauter. Über das verhalten eines elektrons im homogenen elektrischen feld nach der relativistischen theorie diracs. *Zeitschrift für Physik*, 69(11):742–764, Nov 1931.

[3] Werner Heisenberg and Heinrich Euler. Folgerungen aus der diracschen theorie des positrons. *Zeitschrift für Physik*, 98(11):714–732, 1936.

[4] V Weisskopf. Über die elektrodynamik des vakuums auf grund der quantentheorie des elektrons. *Mat. Fys. Medd. Dan Vidensk. Selsk.*, 14(1), 1936.

[5] A Fedotov, A Ilderton, F Karbstein, Ben King, D Seipt, H Taya, and Greger Torgrimsson. Advances in qed with intense background fields. *Physics Reports*, 1010:1–138, 2023.

[6] Jin Woo Yoon, Yeong Gyu Kim, Il Woo Choi, Jae Hee Sung, Hwang Woon Lee, Seong Ku Lee, and Chang Hee Nam. Realization of laser intensity over 1023 w/cm2. *Optica*, 8(5):630–635, 2021.

[7] LUXE collaboration, H Abramowicz, M Almanza Soto, M Altarelli, R Aßmann, A Athanasiadis, G Avoni, T Behnke, M Benettoni, Y Benhammou, et al. Technical design report for the luxe experiment. *The European Physical Journal Special Topics*, 233(10):1709–1974,

2024.

[8] V Yakimenko, L Alsberg, E Bong, G Bouchard, C Clarke, C Emma, S Green, C Hast, MJ Hogan, J Seabury, et al. Facet-ii facility for advanced accelerator experimental tests. *Physical Review Accelerators and Beams*, 22(10):101301, 2019.

[9] S.W. Hawking. Particle creation by black holes. *Commun. Math. Phys.*, 43:199–220, 1975.

[10] Anton Ilderton, William Lindved, and Karthik Rajeev. Hawking radiation from the double copy. *arXiv preprint arXiv:2510.25852*, 2025.

[11] Stephen A. Fulling. Nonuniqueness of canonical field quantization in riemannian space-time. *Phys. Rev. D*, 7:2850–2862, May 1973.

[12] P C W Davies. Scalar production in schwarzschild and rindler metrics. *Journal of Physics A: Mathematical and General*, 8(4):609, apr 1975.

[13] W. G. Unruh. Notes on black-hole evaporation. *Phys. Rev. D*, 14:870–892, Aug 1976.

[14] Y. Rosenberg. Optical analogues of black-hole horizons. *Philosophical Transactions of the Royal Society A*, 378(2177):20190232, 2020.

[15] J. Drori, Y. Rosenberg, D. Bermudez, Y. Silberberg, and U. Leonhardt. Observation of stimulated hawking radiation in an optical analogue. *Phys. Rev. Lett.*, 122:010404, Jan 2019.

[16] A. Pandey. A note on analogue semi-classical gravity in (1+1) dimensions. *Gravitation and Cosmology*, 30(2):229–234, June 2024. arXiv:2405.13359 [gr-qc].

[17] A. Pelat, F. Gautier, S. C. Conlon, and F. Semperlotti. The acoustic black hole: A review of theory and applications. *Journal of Sound and Vibration*, 476:115316, 2020.

[18] M. M. Roberts and T. Wiseman. Analog gravity and continuum effective theory of the graphene tight-binding lattice model. *Phys. Rev. B*, 109:045425, Jan 2024.

[19] Yao Wang, Chong Sheng, Yong-Heng Lu, Jun Gao, Yi-Jun Chang, Xiao-Ling Pang, Tian-Huai Yang, Shi-Ning Zhu, Hui Liu, and Xian-Min Jin. Quantum simulation of particle pair creation near the event horizon. *National Science Review*, 7(9):1476–1484, 05 2020.

[20] T. Cheng, Q. Su, and R. Grobe. Introductory review on quantum field theory with space-time resolution. *Contemporary Physics - CONTEMP PHYS*, 51:315–330, 07 2010.

[21] T. Cheng, Q. Su, and R. Grobe. Creation of multiple electron-positron pairs in arbitrary fields. *Phys. Rev. A*, 80:013410, Jul 2009.

[22] D. D. Su, Y. T. Li, Q. Z. Lv, and J. Zhang. Enhancement of pair creation due to locality in bound-continuum interactions. *Phys. Rev. D*, 101:054501, Mar 2020.

[23] C. K. Li, Y. J. Li, Q. Su, and R. Grobe. Phase sensitivity of the pair-creation process in colliding laser pulses. *Phys. Rev. A*, 108:033112, Sep 2023.

[24] M. Alkhateeb, X. Gutiérrez de la Cal, M. Pons, D. Sokolovski, and A. Matzkin. Relativistic time-dependent quantum dynamics across supercritical barriers for klein-gordon and dirac particles. *Phys. Rev. A*, 103:042203, Apr 2021.

[25] X. Gutiérrez de la Cal, M. Alkhateeb, M. Pons, A. Matzkin, and D. Sokolovski. Klein paradox for bosons, wave packets and negative tunnelling times. *Scientific Reports*, 10(1):19225, Nov 2020.

[26] M. Alkhateeb and A. Matzkin. Space-time-resolved quantum field approach to klein-tunneling dynamics across a finite barrier. *Phys. Rev. A*, 106:L060202, Dec 2022.

[27] M. Alkhateeb and A. Matzkin. Evolution of strictly localized states in noninteracting quantum field theories with background fields. *Phys. Rev. A*, 109:062223, Jun 2024.

[28] M. Alkhateeb, X. Gutierrez de la Cal, M. Pons, D. Sokolovski, and A. Matzkin. Relativistic quantum field theory approach to wavepacket tunneling: Lack of superluminal transmission, 2024.

[29] Antonio Ferreiro, Jose Navarro-Salas, and Silvia Pla. Role of gravity in the pair creation induced by electric fields. *Phys. Rev. D*, 98:045015, Aug 2018.

[30] Chiang-Mei Chen, Sang Pyo Kim, I-Chieh Lin, Jia-Rui Sun, and Ming-Fan Wu. Spontaneous Pair Production in Reissner-Nordstrom Black Holes. *Phys. Rev. D*, 85:124041, 2012.

[31] Markus B. Fröb, Jaume Garriga, Sugumi Kanno, Misao Sasaki, Jiro Soda, Takahiro Tanaka, and Alexander Vilenkin. Schwinger effect in de Sitter space. *JCAP*, 04:009, 2014.

[32] Víctor M. Villalba. Creation of spin-1/2 particles by an electric field in de sitter space. *Phys. Rev. D*, 52:3742–3745, Sep 1995.

[33] J. Garriga. Pair production by an electric field in (1+1)-dimensional de Sitter space. *Phys. Rev. D*, 49:6343–6346, 1994.

[34] N.D. Birrell and P.C.W. Davies. *Quantum Fields in Curved Space*. Cambridge University Press, 1982.

[35] Leonard Parker and David J. Toms. *Quantum Field Theory in Curved Spacetime: Quantized Fields and Gravity*. Cambridge University Press, 2009.

[36] Leonard Parker. Particle creation in expanding universes. *Phys. Rev. Lett.*, 21:562–564, 1968.

[37] L.H. Ford. Quantum field theory in curved spacetime. *Rep. Prog. Phys.*, 84:116901, 2021.

[38] K. Fredenhagen and R. Haag. On the derivation of hawking radiation associated with the formation of a black hole. *Commun. Math. Phys.*, 127:273–284, 1990.

[39] L H Ford. Cosmological particle production: a review. *Reports on Progress in Physics*, 84(11):116901, oct 2021.

[40] L. H. Ford and L. Parker. Creation of particles by singularities in asymptotically flat spacetimes. *Physical Review D*, 17(6):1485–1496, March 1978.

[41] L. Parker and S.A. Fulling. Adiabatic regularization of the energy-momentum tensor of a quantized field in homogeneous spaces. *Phys. Rev. D*, 9:341–354, 1974.

[42] Philip Semrén and Greger Torgrimsson. Worldline instantons for nonperturbative particle production by space and time dependent gravitational fields. 8 2025.

[43] Anton Ilderton and Karthik Rajeev. Tunnelling amplitudes and Hawking radiation from worldline QFT. *JHEP*, 10:220, 2025.

[44] E. T. Akhmedov, D. V. Diakonov, and C. Schubert. Complex effective actions and gravitational pair creation. *Phys. Rev. D*, 110(10):105011, 2024.

[45] James P. Edwards and Christian Schubert. Quantum mechanical path integrals in the first quantised approach to quantum field theory. 12 2019.

[46] Christian Schubert. Perturbative quantum field theory in the string inspired formalism. *Phys. Rept.*, 355:73–234, 2001.

[47] John Joseph M. Carrasco, Yaxi Chen, Nicolas H. Pavao, and Aslan Seifi. Nonperturbative double copy: worldline instantons, color thermality, and backreaction. 1 2026.

- [48] Anton Ilderton, William Lindved, and Karthik Rajeev. Hawking radiation from the double copy. 10 2025.
- [49] John Joseph M. Carrasco and Yaxi Chen. The Double-Copy Root of Hawking Thermality. 11 2025.
- [50] Rafael Aoude, Donal O’Connell, Matteo Sergola, and Chris D. White. Hawking Radiation meets the Double Copy. 10 2025.
- [51] François Fillion-Gourdeau, Emmanuel Lorin, and Steve MacLean. Numerical quasiconformal transformations for electron dynamics on strained graphene surfaces. *Physical Review E*, 103(1):013312, 2021.
- [52] X. Antoine, F. Fillion-Gourdeau, E. Lorin, and S. MacLean. Pseudospectral computational methods for the time-dependent dirac equation in static curved space-times. *J. Comput. Phys.*, 407:109280, 2020.
- [53] F. Fillion-Gourdeau, E. Lorin, and A. D. Bandrauk. Numerical solution of the time-dependent dirac equation in coordinate space without fermion-doubling. *Journal of Computational Physics*, 231(2):582–595, 2012.
- [54] Anton Ilderton. Physics of adiabatic particle number in the schwinger effect. *Physical Review D*, 105(1):016021, 2022.
- [55] Gautam Mandal, Anirvan M Sengupta, and Spentra R Wadia. Classical solutions of 2-dimensional string theory. *Modern Physics Letters A*, 6(18):1685–1692, 1991.
- [56] D. Grumiller and R. McNees. Thermodynamics of Black Holes in Two (and Higher) Dimensions. *Journal of High Energy Physics*, 2007(04):074–074, April 2007. arXiv:hep-th/0703230.
- [57] D. Grumiller and R. McNees. Thermodynamics of Black Holes in Two (and Higher) Dimensions. *Journal of High Energy Physics*, 2007(04):074–074, April 2007. arXiv:hep-th/0703230.
- [58] V. Frolov and A. Zelnikov. Nonminimally coupled massive scalar field in a 2D black hole: Exactly solvable model. *Physical Review D*, 63(12):125026, May 2001.
- [59] A. V. Frolov, K. R. Kristjansson, and L. Thorlacius. Global geometry of two-dimensional charged black holes. *Physical Review D*, 73(12):124036, June 2006. arXiv:hep-th/0604041.
- [60] Mohammed Alkhateeb and Alex Matzkin. Microcausality and tunneling times in relativistic quantum field theory. *Physical Review D*, 112(7):076005, 2025.
- [61] RE Wagner, MR Ware, Q Su, and Rainer Grobe. Bosonic analog of the klein paradox. *Physical Review A—Atomic, Molecular, and Optical Physics*, 81(2):024101, 2010.
- [62] M Alkhateeb, X Gutierrez de la Cal, M Pons, D Sokolovski, and A Matzkin. Relativistic quantum field theory approach to electron wave-packet tunneling: A fully causal process. *Physical Review A*, 111(1):012222, 2025.
- [63] R. M. Wald. Dynamics in nonglobally hyperbolic, static space-times. *Journal of Mathematical Physics*, 21(12):2802–2805, 1980.
- [64] J. W. Braun, Q Su, and R Grobe. Numerical approach to solve the time-dependent dirac equation. *Physical Review A*, 59(1):604, 1999.

Appendix A: Dirac equation in curved spacetime

The formulation of the Dirac equation in curved spacetime relies on a smooth curved spacetime having a

Minkowskian tangent space at any point. At each spacetime point one may introduce a local inertial frame in which the metric takes the Minkowski form and local Lorentz symmetry is manifest. The relation between quantities defined in this local Lorentz frame and those defined in an arbitrary curved coordinate system is provided by the tetrad (or vielbein) formalism.

In this appendix we review the construction of a covariant derivative acting on spinor fields in curved spacetime and outline the derivation of the Dirac equation in a generally covariant form. The strategy is to determine the spinor connection by requiring that spinor bilinears transform correctly as tensors under parallel transport. In particular, we will demand that the probability current constructed from a spinor field transforms as a vector under local Lorentz transformations and parallel transport.

Throughout this section, Greek indices (μ, ν, \dots) denote curved spacetime coordinate indices, while Latin indices (a, b, \dots) denote indices associated with the local Lorentz (orthonormal) frame.

1. Tetrads and local inertial frames

At each spacetime point x , one may introduce a local inertial (orthonormal) frame in accordance with the equivalence principle. The tetrad fields $e^\mu_a(x)$ and their inverses $e^a_\mu(x)$ relate tensor components in this local Lorentz frame to those in an arbitrary curved coordinate system. At a given spacetime point, one may choose local inertial coordinates y^a such that the tetrads coincide with the Jacobian matrices

$$e^\mu_a(x) = \left. \frac{\partial x^\mu}{\partial y^a} \right|_x, \quad e^a_\mu(x) = \left. \frac{\partial y^a}{\partial x^\mu} \right|_x. \quad (\text{A1})$$

This identification is purely pointwise and does not imply the existence of a global coordinate transformation; in a generic curved spacetime the tetrad fields are not globally integrable as coordinate derivatives. For a vector j , the components in the two frames are related by

$$j^\mu(x) = e^\mu_a(x) j^a(x), \quad j^a(x) = e^a_\mu(x) j^\mu(x). \quad (\text{A2})$$

The tetrads satisfy the orthonormality relations

$$\begin{aligned} g_{\mu\nu}(x) e^\mu_a(x) e^\nu_b(x) &= \eta_{ab}, \\ \eta_{ab} e^a_\mu(x) e^b_\nu(x) &= g_{\mu\nu}(x), \\ e^\mu_a(x) e^a_\nu(x) &= \delta^\mu_\nu, \\ e^a_\mu(x) e^\mu_b(x) &= \delta^a_b. \end{aligned} \quad (\text{A3})$$

where $\eta_{ab} = \text{diag}(1, -1, -1, -1)$ is the Minkowski metric in the local Lorentz frame.

2. Levi–Civita connection and vector parallel transport

We assume that spacetime is equipped with the Levi–Civita connection, which is torsion-free,

$$\Gamma^\rho_{\mu\nu} = \Gamma^\rho_{\nu\mu},$$

and metric compatible,

$$\nabla_\rho g_{\mu\nu} = 0.$$

The corresponding Christoffel symbols are therefore given by

$$\Gamma^\rho_{\mu\nu} = \frac{1}{2} g^{\rho\sigma} (\partial_\mu g_{\nu\sigma} + \partial_\nu g_{\mu\sigma} - \partial_\sigma g_{\mu\nu}). \quad (\text{A4})$$

The parallel transport of a vector expressed in the coordinate basis takes the form

$$j^\mu(x + dx) = j^\mu(x) - \Gamma^\mu_{\nu\sigma}(x) j^\nu(x) dx^\sigma. \quad (\text{A5})$$

It is often convenient to express vector components in the local Lorentz frame while keeping the spacetime displacement dx^μ in curved coordinates. We therefore introduce a “mixed” parallel transport law,

$$j^a(x + dx) = j^a(x) - \omega^a_{b\sigma}(x) j^b(x) dx^\sigma, \quad (\text{A6})$$

where $\omega^a_{b\sigma}$ is the spin connection associated with the tetrad. The corresponding covariant derivative is

$$\nabla_\sigma j^a = \partial_\sigma j^a + \omega^a_{b\sigma} j^b. \quad (\text{A7})$$

The purpose of introducing this mixed covariant derivative is to relate the parallel transport of vectors in curved spacetime to their transport in the local Lorentz frame. By requiring consistency between these two descriptions, we determine the spin connection $\omega^a_{b\nu}$ in terms of the tetrads and the Christoffel symbols.

3. Spin connection from tetrads

Using the transformation rule (A2), the mixed transport law (A6) can be rewritten in terms of curved indices as

$$\begin{aligned} j^\mu(x + dx) &= e^\mu_a(x + dx) j^a(x + dx) \\ &= j^\mu(x) + \partial_\nu e^\mu_a(x) j^a(x) dx^\nu \\ &\quad - e^\mu_a(x) \omega^a_{b\nu}(x) j^b(x) dx^\nu, \end{aligned} \quad (\text{A8})$$

where we have used

$$e^\mu_a(x + dx) = e^\mu_a(x) + \partial_\nu e^\mu_a(x) dx^\nu. \quad (\text{A9})$$

Comparing Eq. (A8) with the standard coordinate-basis parallel transport (A5) and eliminating j^a , we obtain

$$-\Gamma^\mu_{\nu\sigma} e^\sigma_b = \partial_\nu e^\mu_b - e^\mu_a \omega^a_{b\nu}. \quad (\text{A10})$$

Solving for the spin connection yields

$$\omega^a_{b\nu} = e^a_\mu \partial_\nu e^\mu_b + e^a_\mu e^\sigma_b \Gamma^\mu_{\nu\sigma}. \quad (\text{A11})$$

This is the standard expression for the spin connection in terms of the tetrads and the Levi–Civita connection.

4. Antisymmetry of the spin connection

The spin connection is antisymmetric in its local Lorentz indices. This property follows from metric compatibility in the local frame, or equivalently from the requirement that parallel transport preserves the local Lorentz scalar product.

Consider deleting this proof (it's standard) To demonstrate this explicitly, consider the squared length of a vector after parallel transport:

$$\begin{aligned} j^a(x + dx) \eta_{ab} j^b(x + dx) &= \eta_{ab} j^a(x) j^b(x) \\ &\quad - \eta_{ab} j^a \omega^b_{d\nu} j^d dx^\nu \\ &\quad - \eta_{ab} j^b \omega^a_{c\nu} j^c dx^\nu. \end{aligned} \quad (\text{A12})$$

Since parallel transport preserves lengths, the $\mathcal{O}(dx)$ terms must cancel, implying

$$\eta_{ab} j^a \omega^b_{d\nu} j^d = -\eta_{ab} j^b \omega^a_{c\nu} j^c. \quad (\text{A13})$$

Lowering the first Lorentz index of the spin connection, $\omega_{ad\nu} \equiv \eta_{ab} \omega^b_{d\nu}$, this becomes

$$j^a \omega_{ad\nu} j^d = -j^a \omega_{dav} j^d. \quad (\text{A14})$$

Because $j^a j^d$ is symmetric under $a \leftrightarrow d$, this relation can hold for arbitrary j^a only if

$$\omega_{ad\nu} = -\omega_{dav}. \quad (\text{A15})$$

5. Spinor parallel transport and spinor connection

We now turn to spinor fields. We assume that the parallel transport of a spinor ψ is governed by a matrix-valued connection Ω_ν ,

$$\psi(x + dx) = \psi(x) - \Omega_\nu(x) \psi(x) dx^\nu. \quad (\text{A16})$$

The adjoint spinor $\bar{\psi} = \psi^\dagger \gamma^0$ transforms as

$$\bar{\psi}(x + dx) = \bar{\psi}(x) - \psi^\dagger(x) \Omega_\nu^\dagger(x) \gamma^0 dx^\nu, \quad (\text{A17})$$

while the scalar bilinear

$$S(x) = \bar{\psi}(x) \psi(x) \quad (\text{A18})$$

must transform as a scalar under parallel transport. Requiring $\nabla_\nu S = \partial_\nu S$ implies

$$\Omega_\nu = -\gamma^0 \Omega_\nu^\dagger \gamma^0. \quad (\text{A19})$$

Next, consider the probability current in the local Lorentz frame,

$$j^a(x) = \bar{\psi}(x) \gamma^a \psi(x), \quad (\text{A20})$$

which must transform as a Lorentz vector. Computing its parallel transport using the spinor connection gives

$$j^a(x + dx) = j^a(x) + \bar{\psi}(x) [\Omega_\nu, \gamma^a] \psi(x) dx^\nu. \quad (\text{A21})$$

On the other hand, vector parallel transport requires

$$j^a(x + dx) = j^a(x) - \omega^a{}_{b\nu} j^b(x) dx^\nu. \quad (\text{A22})$$

Equating these expressions yields the well-known condition

$$[\gamma^a, \Omega_\nu] = \omega^a{}_{b\nu} \gamma^b. \quad (\text{A23})$$

A solution consistent with this relation is

$$\Omega_\nu = -\frac{i}{4} \omega_{ab\nu} \sigma^{ab}, \quad (\text{A24})$$

where

$$\sigma^{ab} = \frac{i}{2} [\gamma^a, \gamma^b]. \quad (\text{A25})$$

This expression satisfies the required commutation relation, as may be verified using the gamma-matrix algebra.

6. Dirac equation in curved spacetime

The curved-spacetime gamma matrices are defined by

$$\gamma^\mu(x) \equiv e^\mu{}_a(x) \gamma^a,$$

which ensures that they satisfy the spacetime Clifford algebra $\{\gamma^\mu, \gamma^\nu\} = 2g^{\mu\nu}\mathbb{I}$ and that the Dirac current transforms as a spacetime vector, and the spinor covariant derivative is defined by

$$\nabla_\nu \psi = \partial_\nu \psi + \Omega_\nu \psi. \quad (\text{A26})$$

The Dirac equation in curved spacetime then takes the generally covariant form

$$i\gamma^\nu \nabla_\nu \psi - m\psi = 0, \quad (\text{A27})$$

or explicitly,

$$ie^\nu{}_a \gamma^a (\partial_\nu + \Omega_\nu) \psi - m\psi = 0. \quad (\text{A28})$$

with Ω_ν given by Eq. (A24).

Appendix B: Local conformal flatness of 1+1-dimensional metrics

In this appendix we show that any 1+1-dimensional Lorentzian metric of the form

$$ds^2 = \alpha_1(\tau, \xi) d\tau^2 - \alpha_2(\tau, \xi) d\xi^2, \quad \alpha_1 \geq 0, \quad \alpha_2 \geq 0, \quad (\text{B1})$$

is locally conformally flat. That is, in a suitable local coordinate system (τ', ξ') , the metric can be written as

$$ds^2 = \alpha(\tau', \xi') (d\tau'^2 - d\xi'^2), \quad (\text{B2})$$

with a positive conformal factor α .

Throughout this appendix we work locally on an open set where $\alpha_1(\tau, \xi) > 0$ and $\alpha_2(\tau, \xi) > 0$, so that the metric has Lorentzian signature.

1. Null decomposition

Define the function

$$c(\tau, \xi) := \sqrt{\frac{\alpha_2(\tau, \xi)}{\alpha_1(\tau, \xi)}}. \quad (\text{B3})$$

Then the metric (B1) can be factorized as

$$\begin{aligned} ds^2 &= \alpha_1(\tau, \xi) (d\tau^2 - c(\tau, \xi)^2 d\xi^2) \\ &= \alpha_1(\tau, \xi) (d\tau - c d\xi) (d\tau + c d\xi). \end{aligned} \quad (\text{B4})$$

Introduce the two null 1-forms

$$\omega_- := d\tau - c d\xi, \quad \omega_+ := d\tau + c d\xi, \quad (\text{B5})$$

so that

$$ds^2 = \alpha_1 \omega_- \omega_+. \quad (\text{B6})$$

It remains to seek local coordinates adapted to these null directions.

2. Integrating factors and null coordinates

We look for nonvanishing functions $\mu(\tau, \xi)$ and $\nu(\tau, \xi)$ such that the 1-forms

$$du := \mu \omega_- = \mu (d\tau - c d\xi), \quad dv := \nu \omega_+ = \nu (d\tau + c d\xi), \quad (\text{B7})$$

are exact.

The condition that du and dv be closed, $d(du) = 0$ and $d(dv) = 0$, yields the first-order linear partial differential equations

$$\partial_\xi \mu + \partial_\tau (\mu c) = 0, \quad (\text{B8})$$

$$\partial_\xi \nu - \partial_\tau (\nu c) = 0. \quad (\text{B9})$$

These equations are transport equations along the characteristic curves defined by

$$d\tau = \pm c(\tau, \xi) d\xi, \quad (\text{B10})$$

which coincide with the null curves of the metric. Standard local existence results for first-order linear PDEs ensure that smooth, nonvanishing solutions μ and ν exist in a sufficiently small neighborhood, given appropriate initial data. Consequently, the functions $u(\tau, \xi)$ and $v(\tau, \xi)$ define a local coordinate system.

From (B7) we obtain

$$d\tau - c d\xi = \frac{1}{\mu} du, \quad d\tau + c d\xi = \frac{1}{\nu} dv. \quad (\text{B11})$$

Substituting into (B6) gives

$$ds^2 = \frac{\alpha_1(\tau, \xi)}{\mu(\tau, \xi) \nu(\tau, \xi)} du dv = \theta^2(u, v) du dv, \quad (\text{B12})$$

where

$$\theta^2(u, v) := \frac{\alpha_1(\tau(u, v), \xi(u, v))}{\mu(\tau, \xi) \nu(\tau, \xi)}. \quad (\text{B13})$$

3. Conformally flat coordinates

Finally, define new coordinates (τ', ξ') by

$$\tau' = \frac{v+u}{2}, \quad \xi' = \frac{v-u}{2}. \quad (\text{B14})$$

A direct computation shows that

$$du\,dv = d\tau'^2 - d\xi'^2. \quad (\text{B15})$$

Therefore, the metric (B12) becomes

$$ds^2 = \theta^2(u, v) (d\tau'^2 - d\xi'^2). \quad (\text{B16})$$

Defining

$$\alpha(\tau', \xi') := \theta^2(u(\tau', \xi'), v(\tau', \xi')), \quad (\text{B17})$$

we arrive at the conformally flat form

$$ds^2 = \alpha(\tau', \xi') (d\tau'^2 - d\xi'^2). \quad (\text{B18})$$

This completes the proof of the well-known fact that any 1+1-dimensional Lorentzian metric of the form (B1) is locally conformally flat.